

## Nanocrystalline $\alpha$ -Al<sub>2</sub>O<sub>3</sub> powder preparation with sucrose as a template through a chemical route

Rifki Septawendar\*, Suhanda and Frank Edwin

Researchers at Department of Advanced Ceramic, Glass, and Enamel, Center for Ceramics, Ministry of Industry of Indonesia, Jl. Akhmad Yani, No. 392, Bandung 40272, West Java, Indonesia

Nanocrystalline  $\alpha$ -Al<sub>2</sub>O<sub>3</sub> powder was prepared through a chemical route via a reaction between aluminum nitrate nona hydrate with a sucrose template in variation ratios of the salt to the organic namely 1 : 2, 3 : 1, and 6 : 1 at a heating temperature of 200 °C. The homogenization process of the nanopowder was assisted by milling a "charcoal precursor" in a non polar solvent for 24 hours, which was then successfully calcined at temperatures of 900 °C and 1100 °C. The products were evaluated by X-ray diffraction (XRD) analysis, scanning electron microscopy (SEM) and transmission electron microscopy (TEM). The optimum condition was obtained at a ratio of the aluminum salt to the organic compound of about 6 : 1, at a calcination temperature of 900 °C, which produced a 100% pure  $\alpha$ -Al<sub>2</sub>O<sub>3</sub> phase with a crystallite size of 44.6 nm. The SEM micrographs showed the particle sizes of nanocrystalline  $\alpha$ -Al<sub>2</sub>O<sub>3</sub> powders were found to be near 100 nm at 1100 °C. The TEM results indicate that nanocrystalline  $\alpha$ -Al<sub>2</sub>O<sub>3</sub> powders calcined at 900 °C had grain sizes below 50 nm. An increase of the sucrose concentration leads to smaller crystal sizes, meanwhile an elevation of the calcination temperature from 900 °C to 1100 °C leads to the formation of larger particle and crystal sizes of alumina.

**Key words:** Nanocrystalline, Al<sub>2</sub>O<sub>3</sub>, Sucrose, A chemical process, Calcination temperature.

### Introduction

Alumina (Al<sub>2</sub>O<sub>3</sub>) shows excellent physical and chemical properties, including the highest strength among oxides, excellent abrasion resistance, heat resistance, a high dielectric strength at high voltage, and high resistance to chemical attack (See in Table 1) [1-3]. Therefore, these characteristics enable Al<sub>2</sub>O<sub>3</sub> to have been widely used in many applications as presented in Table 2 [2-6].

These applications demand a particular nano-sized powder, so that nano-sized alumina powders will be indispensable for the manufacturing of various advanced materials and devices in the future [7]. The synthesis of materials of nanometre dimensions can access new material properties and device characteristics in unprecedented ways. Controlled structures, large interfaces, power density and other unique characteristics are examples of the superiority of nanomaterial properties that will improve their properties and functionalities [8-11].

Many methods have been used to synthesize alumina either with submicrometre or nano dimensions via a chemical route [12, 13], namely: Sarikaya and Akinc [14], prepared alumina microshells by calcining the precursor with an emulsion evaporation technique; on the other hand, Lin and Wen [15], used a chemical precipitation method to prepare an alumina precursor via an emulsified boehmite

**Table 1.** Some Mechanical, Thermal, and Electrical Properties of 99.8% Al<sub>2</sub>O<sub>3</sub> [1, 2]

Property (Condition, Unities)	Value
Bulk density (20 °C, g/cm <sup>3</sup> )	3.96
Tensile strength (20 °C, MPa)	220
Bending strength (20 °C, MPa)	410
Elastic modulus (20 °C, GPa)	375
Hardness (20 °C, MPa)	137.293
Fracture toughness (20 °C, MPa·m <sup>1/2</sup> )	4-5
Porosity (20 °C, %)	0
Maximum working temperature (°C)	1700
Thermal expansion coefficient (10 <sup>6</sup> /°C)	
25-300 °C:	7.8
25-1000 °C:	8.1
Thermal conductivity (20 °C, W/m K)	28
Dielectric constant (1 MHz)	9.7
20 °C:	> 10 <sup>14</sup>

**Table 2.** Alumina functional ceramic and its applications [2-6]

No	Function	Application
1	Electronic function	IC-Board, Resistor substrates, Electron tube, and others
2	Optical function	High pressure sodium lamp non- volatile memory window
3	Chemical functions	Temperature sensor, catalytic converter, organic catalyst
4	Mechanical functions	Mechanical seals, ceramic liner
5	Biological function	Artificial teeth, artificial joints, artificial bones

\*Corresponding author:  
Tel : +6285624249484  
Fax: +6222 7205322  
E-mail: rifkiseptawendar@yahoo.com

gel with oleic acid. Lee *et al.* [7], prepared nanoalumina powder by calcining an emulsion precursor derived from an aqueous  $\text{Al}(\text{NO}_3)_3$  solution that was mixed with oleic acid. Bastomi *et al.* [16], synthesized submicrometre  $\alpha\text{-Al}_2\text{O}_3$  using the precursor process method. Pati *et al.* [17], prepared nanocrystalline  $\alpha\text{-Al}_2\text{O}_3$  powder at  $1150^\circ\text{C}$  for 2 h by the pyrolysis of a precursor material prepared by evaporation of an aqueous solution of sucrose with polyvinyl alcohol and a metal nitrate. Peng *et al.* [18], synthesized  $\alpha\text{-Al}_2\text{O}_3$  by combustion synthesis using glycine as the fuel and a nitrate as an oxidizer. Ding *et al.* [19], synthesized  $\alpha\text{-Al}_2\text{O}_3$  at  $1250^\circ\text{C}$  via the reaction:  $2\text{AlCl}_3 + 3\text{CaO} \rightarrow \text{Al}_2\text{O}_3 + 3\text{CaCl}_2$ . Pati *et al.* [20], prepared nanocrystalline  $\alpha\text{-Al}_2\text{O}_3$  powders at  $1025^\circ\text{C}$  by the pyrolysis of a complex compound of aluminum with triethanolamine (TEA) and the final material had particles 25 nm in size.

According to the previous researches,  $\alpha\text{-Al}_2\text{O}_3$  was formed at quite high temperatures from  $1000$  to  $1100^\circ\text{C}$  [1, 2, 4, 14-20]. The purposes of this study are to synthesize nanocrystalline  $\alpha\text{-Al}_2\text{O}_3$  powders at a lower temperature of  $900^\circ\text{C}$ , and to investigate the effects of a sucrose and the calcination temperature on the phase transformation and crystal size of  $\alpha\text{-Al}_2\text{O}_3$  formed. The higher sucrose concentration used is assumed to produce a smaller crystal size of  $\alpha\text{-Al}_2\text{O}_3$ . Alumina starting materials used are  $\text{Al}^{3+}$  cations of aluminum salts ( $\text{Al}(\text{NO}_3)_3 \cdot 9\text{H}_2\text{O}$ ), having a very small size of  $0.53$  nm. The cations are then coated by sucrose to restrict faster growth of crystals, thus obstructing the formation of larger crystals. Therefore, at below a calcination temperature of  $1000^\circ\text{C}$ , it is assumed that  $\alpha\text{-Al}_2\text{O}_3$  would be formed as very small crystals. In this study, the calcination temperatures were  $900^\circ\text{C}$  and  $1100^\circ\text{C}$ , whereas a calcination temperature of  $1100^\circ\text{C}$  was a reference based on the previous research. Fig. 1 shows a flowchart of nanocrystalline  $\alpha\text{-Al}_2\text{O}_3$  powder preparation from an aluminum salt via a chemical route.

## Experimental Procedure

Alumina precursors were initially prepared by mixing and dissolving an aluminum salt with sucrose into demineralized water and stirring the mixture approximately at a speed of  $800$  rpm. The process was conducted until a brown gel formed. The weight ratios of the aluminum salt to sucrose were in the ranges of about  $6:1$ ,  $3:1$ , and  $1:2$ . At the time of mixing, a  $5$  M ammonia solution was added slowly into the mixture until hydrolysis occurred along with the stirring and heating process. The gel produced was stirred and heated on a hot plate at a temperature of  $200^\circ\text{C}$  to remove water and to produce a charcoal precursor at the end of mixing-heating process. Charcoal or the alumina precursor was milled and homogenized in a non polar solvent for 24 hours, and then it was successfully calcined in a furnace at the temperatures of  $900^\circ\text{C}$ , and  $1100^\circ\text{C}$ . The final product was then characterized.

The crystalline phase and average crystallite size of the calcined powder were determined by X-ray diffraction (XRD

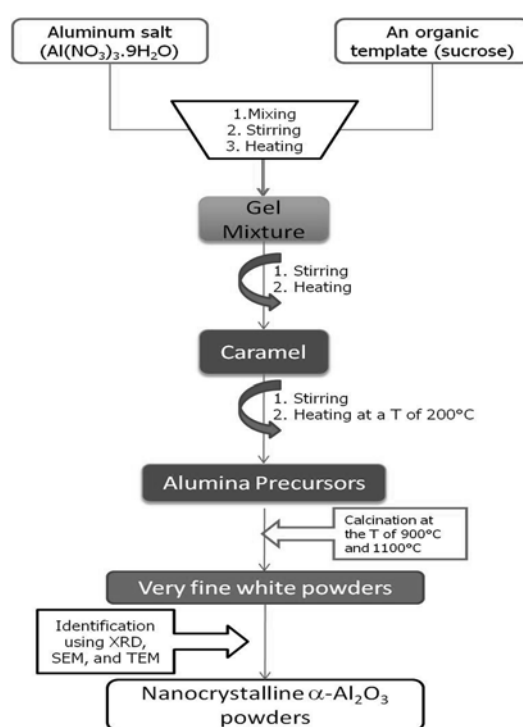


**Fig. 1.** A flowchart of nanocrystalline  $\text{Al}_2\text{O}_3$  powder preparation through a chemical route via a reaction between aluminum nitrate nona hydrate with a sucrose template.

Merck Phillips PW 3710 mpd control with a Cu target). A scanning electron microscope (SEM, JEOL JSM-35C) was used to investigate the particle size and morphology. A transmission electron microscope (TEM, JEOL) was performed to verify the grain size.

## Results and Discussion

### The results of XRD analysis

*Alumina phase transformation based on the XRD qualitative analysis*

In alumina nano powder preparation via a chemical reaction, diffraction patterns of the precursor alumina for all the compositions after calcination at temperatures of  $900^\circ\text{C}$  and  $1100^\circ\text{C}$  with a soaking time for 5 hours are presented in Figs. 2 and 3. X-rays diffraction analysis indicates that  $\gamma\text{-Al}_2\text{O}_3$  and ( $\alpha\text{-Al}_2\text{O}_3$ ) corundum are formed for the compositions of  $3:1$  and  $1:2$  at a temperature of  $900^\circ\text{C}$  with overlapping and broadened peaks in the diffractogram. This is expected to have a particle size which is smaller than previously obtained. Meanwhile,  $\alpha\text{-Al}_2\text{O}_3$  corundum is the only phase formed for a composition of  $6:1$  at a temperature of  $900^\circ\text{C}$ . At a higher calcination temperature of  $1100^\circ\text{C}$ ,  $\alpha\text{-Al}_2\text{O}_3$  is the only phase formed for all the compositions. Thus, the crystal phase transformation of alumina occurring is aluminum hydroxide  $\rightarrow$  boehmite  $\rightarrow$   $\gamma\text{-Al}_2\text{O}_3$  (cubic)  $\rightarrow$   $\alpha\text{-Al}_2\text{O}_3$  (trigonal/ rhombohedral).

The peak patterns in the diffractograms for the compositions of AN  $1:2$  and AN  $3:1$  at  $900^\circ\text{C}$  are broad, thus indicating

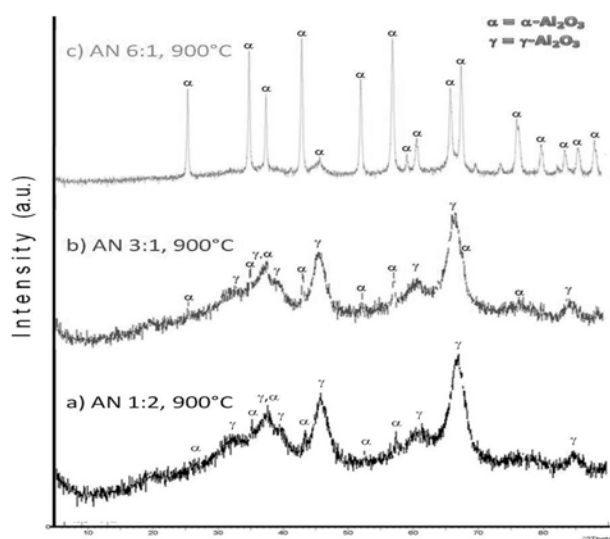


Fig. 2. XRD diffraction patterns of alumina for all the compositions at a temperature of 900 °C.

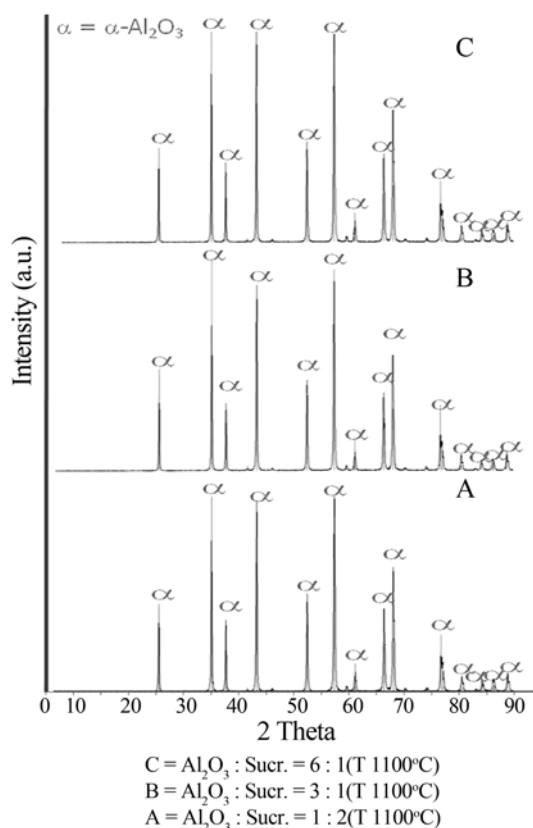


Fig. 3. XRD diffraction patterns of alumina for all the compositions at a temperature of 1100 °C.

the synthesized nanocrystalline  $\alpha$ - $\text{Al}_2\text{O}_3$  powders have a very fine crystallite size. The existence of the main diffraction peaks in certain crystal planes emphasizes that synthesized  $\text{Al}_2\text{O}_3$  powders are crystalline not amorphous [21].

*The XRD quantitative analysis for measuring crystallite sizes and determining alumina phase concentrations*

A quantitative analysis of diffractogram patterns for each

sample including crystallite sizes and concentration of alumina phases formed was applied and assisted using XRD software.

Nevertheless, a quantitative analysis could not be applied directly for the XRD results of AN 1 : 2 and AN 3 : 1 compositions at 900 °C because of their low intensity peaks, in which they can not be resolved because of peak broadening and overlapping. Therefore, JCPDS 10-0425 ( $\gamma$ - $\text{Al}_2\text{O}_3$ ) and JCPDS 83-2080 ( $\alpha$ - $\text{Al}_2\text{O}_3$ ) databases were used as references or standards in determining crystallite sizes and concentration of the alumina phases formed. Thus, before calculating the crystallite size, the peak patterns in each sample diffractogram were initially corrected by subtracting and fitting the corresponding peak patterns with standard peak patterns in JCPDS 10-0425 ( $\gamma$ - $\text{Al}_2\text{O}_3$ ) and JCPDS 83-2080 ( $\alpha$ - $\text{Al}_2\text{O}_3$ ), which was assisted by XRD software [21]. The average crystallite size was calculated using the Scherrer equation [22]:

$$D = \frac{\kappa\lambda}{\beta \cos\theta} \quad (1)$$

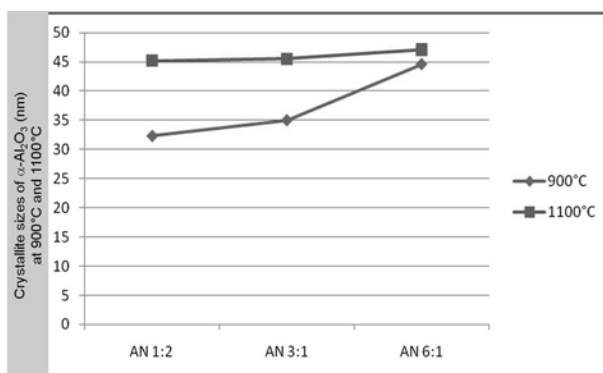
where  $D$  is the crystallite size,  $K$  is a shape factor with a value of 0.9-1.4,  $\lambda$  is the wavelength of the X-rays (1.54056 Å),  $\theta$  is Bragg's angle and  $\beta$  is the value of the full width at half maximum (radian). Table 3 presents the quantification results of these alumina samples using the Rietveld and the Scherrer methods on aluminum oxide phases.

According to the data in Table 3, in general, it practically gives a linear correlation with an increase of the sucrose concentration, and an elevation of the calcination temperature. The higher the sucrose concentration that is used at the temperatures of 900 °C and 1100 °C, the smaller the crystal size will be produced (Fig. 4(a)). This is because the sucrose is distributed and spread evenly on the salt surfaces so that either the binding distance or particle density will be wider; and in the calcination step, this would give a chance of forming smaller crystals. However, a decrease of the sucrose concentration leads to a higher concentration of the  $\alpha$ - $\text{Al}_2\text{O}_3$  phase at 900 °C, according to the data in Table 3 and a curve in Fig. 4(b). Based on Table 3, the optimum condition was obtained at a ratio of the aluminum salt to the organic compound of about 6 : 1, at a calcination temperature of 900 °C, which produced 100% pure  $\alpha$ - $\text{Al}_2\text{O}_3$  phase with crystallite size of 44.6 nm in size.

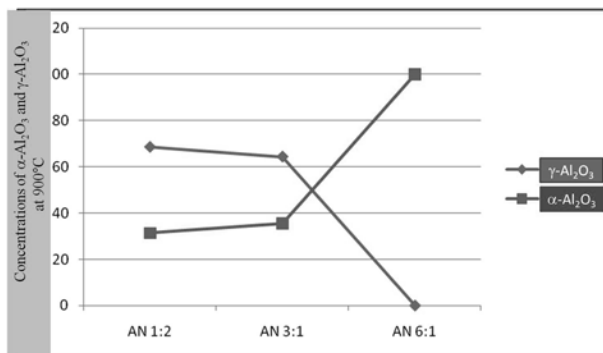
The ratio of the aluminium salt to sucrose template concentration is very important in nanocrystalline  $\alpha$ - $\text{Al}_2\text{O}_3$  preparation. The crystal or particle size produced from a ratio of the aluminum salt to the template, such as 1 : 2 (% wt) will be smaller than the crystal or particle size produced when the ratios of the aluminum salt to the template are 3 : 1, and 6 : 1. This is caused by the concentration of  $\text{Al}^{3+}$  ions of the precursor with a greater amount of sucrose will be lower during the course of the phase transformation. As the calcination temperature is increased, the material is considered to be deficient in  $\text{Al}^{3+}$  content so that this retards the crystallite grain growth. With an excess sucrose

**Table 3.** Quantitative results from the Rietveld and the Scherrer methods of aluminum oxide phases

No	Sampel code (salt:sucrose)	Calcination temperature (°C)	Dominant mineral phase (% Concentration)	Average Crystallite size (nm)	PDF No.
1	AN 1 : 2	900	Cubik $\gamma$ -Al <sub>2</sub> O <sub>3</sub> (68.6%) Trigonal $\alpha$ -Al <sub>2</sub> O <sub>3</sub> (31.4%)	5,8 32,3	10-0425 83-2080
2	AN 3 : 1	900	Cubik $\gamma$ -Al <sub>2</sub> O <sub>3</sub> (64.4%) Trigonal $\alpha$ -Al <sub>2</sub> O <sub>3</sub> (35.6%)	6,3 35	10-0425 83-2080
3	AN 6 : 1	900	Trigonal $\alpha$ -Al <sub>2</sub> O <sub>3</sub> (100%)	44,6	83-2080
4	AN 1 : 2	1100	Trigonal $\alpha$ -Al <sub>2</sub> O <sub>3</sub> (100%)	45,2	83-2080
5	AN 3 : 1	1100	Trigonal $\alpha$ -Al <sub>2</sub> O <sub>3</sub> (100%)	45,5	83-2080
6	AN 6 : 1	1100	Trigonal $\gamma$ -Al <sub>2</sub> O <sub>3</sub> (100%)	47,1	83-2080



(a)



(b)

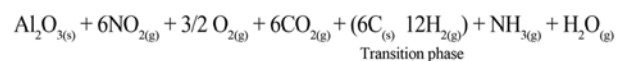
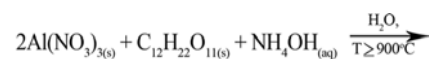
**Fig. 4.** (a) A correlation curve between weight concentration ratios of sucrose to the crystallite size of  $\alpha$ -Al<sub>2</sub>O<sub>3</sub> (nm), at 900 °C and 1100 °C (b) A correlation curve between weight concentration ratios of sucrose to the concentration of  $\alpha$ -Al<sub>2</sub>O<sub>3</sub> formed (%) at 900 °C.

concentration, this masking compound will be completely distributed on the salt surfaces so that the binding distance or particle density will be wider, because sucrose restricts the grain contact among the nucleated  $\alpha$ -Al<sub>2</sub>O<sub>3</sub> and restrains the crystallite growth [3].

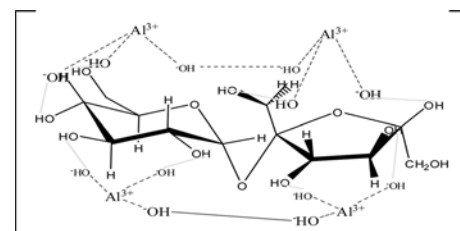
An organic template, in this case sucrose, is not only capable of masking salt molecules on the surface, but also forms “aluminum-sucronate” in the condition of a free from water solvent (mechanical water), especially at a temperature condition above 100 °C. The product transition from the reaction between sucrose and aluminum salt (*nitrate*/

sulphate) after heating slowly at that temperature along with the addition of ammonia is assumed to produce a metal organic compound of aluminum sucronate. When the product was calcined at a higher temperature, it would produce aluminum oxide, CO<sub>2(g)</sub>, 6C<sub>(s)</sub>, H<sub>2(g)</sub>, NO<sub>2(g)</sub>, O<sub>2(g)</sub>, NH<sub>3(g)</sub>, and H<sub>2</sub>O.

In the case of the preparation of nanocrystalline alumina powders from an aluminum salt, the reactions are assumed as follows:

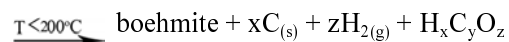
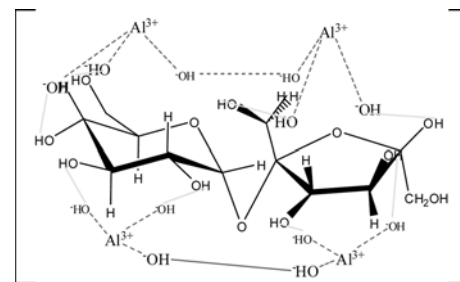


1.....Step 1, at a temperature of  $\leq 100$  °C with stirring  
 $n \text{Al}(\text{OH})_{3(aq)} + m \text{sucrose}_{(aq)} \xrightarrow{\text{T} \leq 100^\circ\text{C}}$

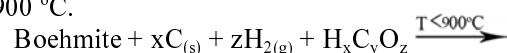


“Aluminum sucronate” (brown gel)

2.....Step 2, at a temperature above 200 °C with stirring



3.....Step 3, at a calcination temperature above 900 °C.





### Morphology and Microstructure

According to the SEM micrographs as presented in Fig. 5, the sizes of the  $\alpha$ - $\text{Al}_2\text{O}_3$  powders were found to be near 100 nm at 1100 °C and illustrate the formation of sintering necks and interconnection among grains. As the template content decreased, the crystalline grains grown substantially; more sintering necks and interconnections were formed. Typical TEM images of  $\alpha$ - $\text{Al}_2\text{O}_3$  powders for (salt/sucrose) masking gel ratios (a) 3 : 1, (b) 1 : 2 (Fig. 6) show that the grain sizes were in the range below 50 nm and the electron diffraction (ED) patterns of the composition of 3 : 1 is indexed to rhombohedral  $\alpha$ - $\text{Al}_2\text{O}_3$  with the crystal plane orientations of [012] and [113]. This ED result corroborates the XRD result for the composition ratio 3 : 1, which showed the formation of  $\gamma$ - $\text{Al}_2\text{O}_3$  and  $\alpha$ - $\text{Al}_2\text{O}_3$  (corundum) phases.

The size of the nano  $\alpha$ - $\text{Al}_2\text{O}_3$  product is sensitive to the calcination temperature and the concentration of the sucrose template in the feedstock for preparation [3].

However, the above results indicate that the overall process represents an effective methodology and has a commercial aspect; nevertheless, further experiments are

needed to provide more comprehensive results for a full understanding of the preparation process of nanocrystalline alumina powders.

### Conclusions

The size of nano  $\alpha$ - $\text{Al}_2\text{O}_3$  is sensitive to the concentration of the sucrose template for preparation and the calcination temperature. In general, an increase of the sucrose concentration leads to smaller crystal sizes, meanwhile an elevation of the calcination temperature from 900 °C to 1100 °C leads to the formation of larger particle and crystal sizes of alumina.

The optimum conditions were obtained at a ratio of the aluminum salt to the organic compound of about 6 : 1, at a calcination temperature of 900 °C, which produced 100% pure  $\alpha$ - $\text{Al}_2\text{O}_3$  phase with a crystallite size of 44.6 nm in size. The SEM micrographs show the particle sizes of nanocrystalline  $\alpha$ - $\text{Al}_2\text{O}_3$  powders were found to be near 100 nm at 1100 °C. The TEM results indicate that nanocrystalline  $\alpha$ - $\text{Al}_2\text{O}_3$  powders calcined at 900 °C had grain sizes below 50 nm.

The experimental results indicate that the overall process represents an effective methodology and has a commercial aspect for the preparation of nanocrystalline  $\alpha$ - $\text{Al}_2\text{O}_3$  powders.

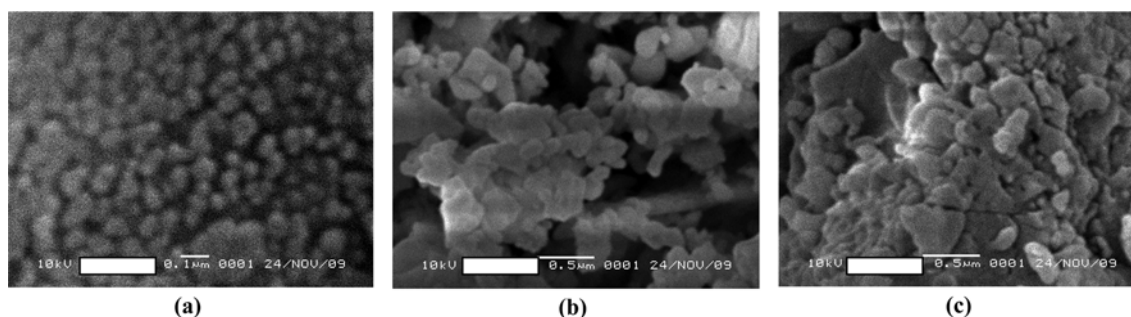


**Fig. 5.** SEM images of  $\alpha$ - $\text{Al}_2\text{O}_3$  powders obtained after calcination at a temperature of 1100 °C for 5 hours for the compositions of (a) 1 : 2, (b) 3 : 1, and c) 6 : 1, respectively.

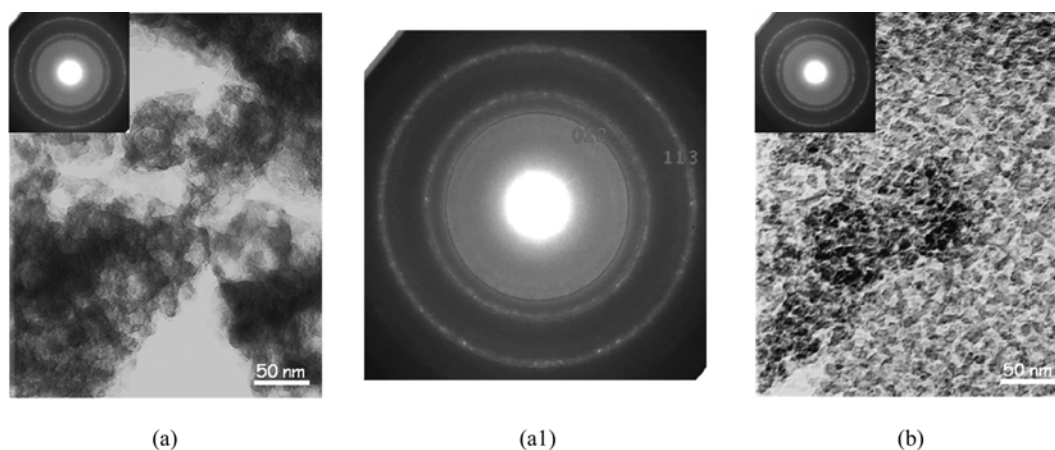


**Fig. 6.** TEM images of  $\alpha$ - $\text{Al}_2\text{O}_3$  powders obtained after calcination at a temperature of 900 °C for 5 hours for the compositions of (a) 3 : 1, and (b) 1 : 2, respectively; and ED pattern of composition of 3 : 1-900 °C (a1).

## References

1. J.A. Rodriguez and M.F. Garcia, *Synthesis, Properties, and Applications of Oxide Nanomaterials*, Wiley Interscience, New Jersey, (2007).
2. Y. Lee, Y.M. Hahm and D.-H. Lee, *J. Ind. Eng. Chem.*, 10[5] (2004) 826-833.
3. N. Ichinose, K. Komeya, N. Ogino, A. Tsuge and Y. Yokomizo, *Introduction To Fine Ceramics. Applications In Engineering*, John Wiley & Sons, New York, (1987).
4. P.S. Santos, H.S. Santos and S. P. Toledo, *Mater. Res.*, 3[4] (2000) 104-114.
5. G. Paglia. "Determination of the Structure of  $\gamma$ -Alumina using Empirical and First Principles Calculations Combined with Supporting Experiments". Curtin University of Technology, (2004).
6. H. Kaga and R. Koc, *J. Am. Ceram. Soc.* 90[6] (2007) 1723-1727.
7. Y.-C. Lee, S.-B. Wen and L. Wenglin, *J. Am. Ceram. Soc.* 90[6] (2007) 1723-1727.
8. M.C. Roco and W.S. Bainbridge, in *NSET Workshop Report of "Societal Implications of Nanoscience and Nanotechnology*, National Science Foundation, Virginia, March (2001).
9. R.W. Siegel, E. Hu and M.C. Roco, in *Proceedings of the May 8-9, 1997 Workshop on "R&D Status and Trends in Nanoparticles, Nanostructured Materials, and Nanodevices in the United States"*, May 8-9, Baltimore, Maryland, (1998) p. 1-3
10. The Royal Society & The Royal Academy of Engineering, *Nanoscience and nanotechnologies: opportunities and uncertainties*, London, (2004), Retrieved 2008-05-18.
11. G. Cao, *Nanostructures & Nanomaterials: Synthesis, Properties, & Applications*. Imperial College Press, USA, (2004).
12. A.K. Bandyopadhyay. *Nano Materials*. New Age International, New Delhi, (2008).
13. K.C. Patil, M.S. Hedge, T. Rattan and S.T. Aruna, *Chemistry of Nanocrystalline Oxide Materials, Combustion Synthesis, Properties and Applications*, World Scientific, New Jersey, (2008).
14. Y. Sarikaya and M. Akinc, *Ceram Int.* 14[4] (1988) 239-244.
15. C.P. Lin and S.B. Wen, *J. Am. Ceram. Soc.*, 85[6] (2002) 1467-72.
16. T. Bastomi, B.S. Purwasasmita and R. Septawendar, in *Proceeding of Ceramic National Seminar VIII, "The Development of Ceramic Research Result through A Collaboration with Industries To Improve The Competitiveness and The Added Value of The Industrial Products"*, May 27, Savoy Homan, West Java, Indonesia, (2009), p.99-104.
17. R.K. Pati, J.C. Ray and P. Pramanik, *Mater. Lett.*, 44[5] (2000) 299-303.
18. T. Peng, X. Liu, K. Dai, J. Xiao and H. Song, *Mater. Res. Bull.*, 41[9] (2006) 1638-1645.
19. J. Ding, T. Tsuzuki and P.G. McCormick, *J. Am. Ceram. Soc.*, 79[11] (1996) 2956-2958.
20. R.K. Pati, J.C. Ray and P. Pramanik, *J. Am. Ceram. Soc.*, 84[12] (2004) 2849-2852.
21. Y. Zhou, N. Dasgupta and A.V. Vikrar, *J. Am. Ceram. Soc.*, 91[3] (2008) 1009-1012.
22. Y.J. Kwon, K.H. Kim, C.S. Lim and K.B. Shim, *J. Ceram. Proc. Res.*, 3[3] (2002) 146-149.